

Article

Understanding the Origin of the Regioselectivity in Non-Polar [3+2] Cycloaddition Reactions through the Molecular Electron Density Theory

 Luis R. Domingo ^{1,*} , Mar Ríos Gutiérrez ^{1,2,*}  and Jorge Castellanos Soriano ³ 
¹ Department of Organic Chemistry, University of Valencia, Dr. Moliner 50, Burjassot, 46100 Valencia, Spain

² Department of Chemistry and Chemical Biology, McMaster University, 1280 Main Street West, Hamilton, ON L8S 4L8, Canada

³ Department of Chemistry, Polytechnic University of Valencia, Camí de Vera, s/n, 46022 Valencia, Spain; jorcass1@qim.upv.es

* Correspondence: domingo@utopia.uv.es (L.R.D.); rios@utopia.uv.es (M.R.G.)

Received: 5 September 2020; Accepted: 10 November 2020; Published: 13 November 2020

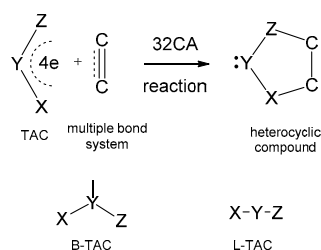


Abstract: The regioselectivity in non-polar [3+2] cycloaddition (32CA) reactions has been studied within the Molecular Electron Density Theory (MEDT) at the B3LYP/6-311G(d,p) level. To this end, the 32CA reactions of nine simplest three-atom-components (TACs) with 2-methylpropene were selected. The electronic structure of the reagents has been characterized through the Electron Localisation Function (ELF) and the Conceptual DFT. The energy profiles of the two regioisomeric reaction paths and ELF topology of the transition state structures are studied to understand the origin of the regioselectivity in these 32CA reactions. This MEDT study permits to conclude that the least electronegative X1 end atom of these TACs controls the asynchronicity in the C–X (X=C, N, O) single bond formation, and consequently, the regioselectivity. This behaviour is a consequence of the fact that the creation of the non-bonding electron density required for the formation of the new single bonds has a lower energy demand at the least electronegative X1 atom than at the Z3 one.

Keywords: non-polar [3+2] cycloaddition reactions; regioselectivity; molecular electron density theory; electronegativity; molecular mechanism

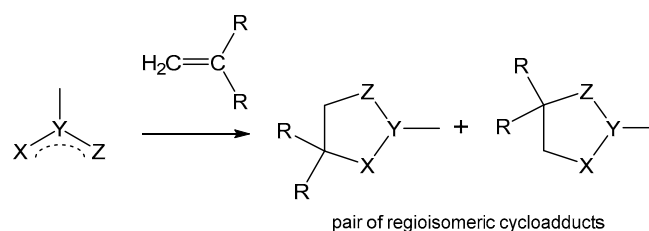
1. Introduction

Cycloaddition reactions are one of the most useful tools in organic synthesis as they permit to obtain cyclic organic compounds with a regio- and/or stereoselective fashion [1,2]. [3+2] cycloaddition (32CA) reactions are an important class of cycloaddition allowing the formation of five-membered heterocycles of great pharmaceutical and industrial interest [3,4]. This kind of cycloaddition implies the 1,3-addition of an ethylene derivative to a three-atom-component (TAC) (see Scheme 1). Depending on its structure, TACs can be classified as bent TACs (B-TACs) or linear TACs (L-TACs).



Scheme 1. 32CA reaction scheme and simplified Lewis structure of bent (B) and linear (L) TACs.

Many of the TACs participating in 32CA reactions are non-symmetric with respect to the central atom. When ethylenes, such as 1-substituted or 1,1-disubstituted ethylenes, are also non-symmetric, at least a pair of regioisomeric cycloadducts can be formed along the reaction (see Scheme 2). Unlike Diels–Alder (DA) reactions, which are highly regioselective yielding a single cycloadduct [5], 32CA reactions are not as selective, yielding a mixture of the two feasible regioisomers. As regioisomers are structural isomers with physical and chemical different properties, only one of them will have a synthetic interest; consequently, formation of a mixture of two regioisomers involves a loss of the synthetic yield. Thus, the understanding of the origin of the regioselectivity in 32CA reactions is an important goal in order to predict the formation of reaction mixtures.



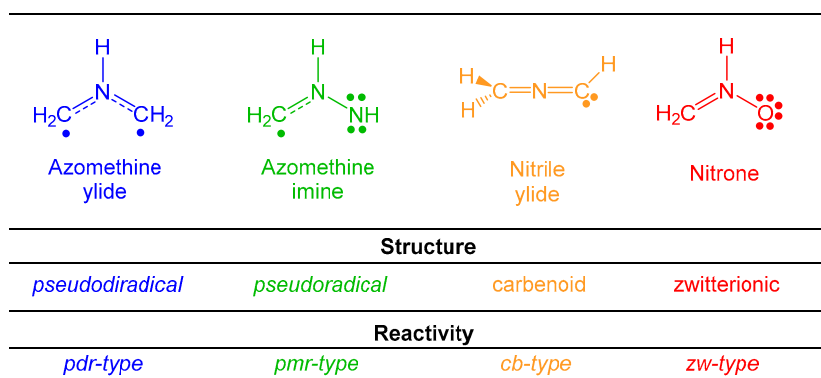
Scheme 2. Formation of regioisomeric cycloadducts in 32CA reactions involving non-symmetric reagents.

The regioselectivity of polar 32CA reactions was investigated in 2004 [6] by using the global and local reactivity indices defined within the Conceptual DFT (CDFT) [7,8]. That study suggested that for asynchronous 32CA reactions associated to polar processes, the regioselectivity is consistently explained by the most favourable two-centre interaction between the most nucleophilic and electrophilic sites of the reagents [6]. While the analysis of the electrophilicity [9] ω and nucleophilicity [10] N indices allows characterizing the chemical properties of the reagents participating in polar processes, analysis of the Parr functions [11] allows characterizing the most electrophilic and nucleophilic centres of a molecule. However, unlike DA reactions, many 32CA reactions have low polar character, even non-polar, and consequently, the polar model to predict regioselectivity fails in this type of cycloaddition reactions.

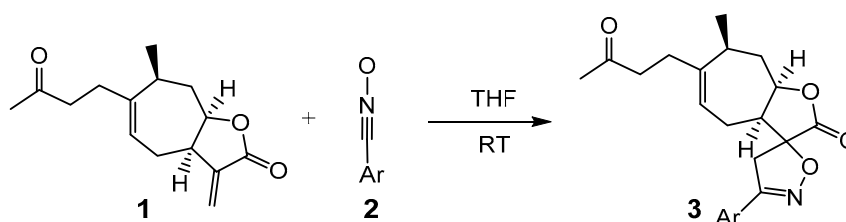
In 2016, Domingo proposed the Molecular Electron Density Theory [12] (MEDT) for the study of the reactivity in Organic Chemistry, in which changes in the electron density, and not MO interactions, as the Frontier Molecular Orbital (FMO) theory proposed [13], are responsible for the feasibility of an organic reaction. Accordingly, in MEDT, several quantum-chemical tools based on the analysis of the electron density, such as the analysis of the CDFT reactivity indices [7,8], the topological analysis of the Electron Localisation Function (ELF) [14] and the Quantum Theory of Atoms in Molecules (QTAIM) [15], are used to rigorously study the chemical reactivity in Organic Chemistry [12].

Recent advances made in the theoretical understanding of 32CA reactions based on MEDT have allowed establishing a very good correlation between the electronic structure of the simplest TACs and their reactivity towards ethylene [16]. Accordingly, depending on the electronic structure of the simplest TACs, *pseudodiradical*, *pseudoradical*, carbenoid and zwitterionic, 32CA reactions have been classified into *pseudodiradical-type* (*pdr-type*), *pseudomonoradical-type* (*pmr-type*), carbenoid-type (*cb-type*) and zwitterionic-type (*zw-type*) reactions [16], respectively, in such a manner that while *pdr-type* 32CA reactions can be carried out very easily, *zw-type* 32CA reactions demand adequate nucleophilic/electrophilic activations to take place (see Scheme 3).

These findings have provided a rationalisation of experimental outcomes [17–21]. In 2017, Zaki and co-workers reported the synthesis of a series of enantiomerically pure isoxazolines by 32CA reactions of substituted aryl nitrile oxides **2** with tomentosin **1**, a sesquiterpene lactone extracted from *Dittrichia viscosa* (see Scheme 4) [22]. The interest of this reaction was that, although tomentosin **1** presents up to sixteen different approach modes associated with two regio- and two diastereofacial reaction paths for each of the four C–C and C–O double bond systems, only one product was isolated under smooth conditions. Thus, when benzonitrile oxide (**2**, Ar=Ph) was used, the corresponding spiro-isoxazoline **3** was obtained in 72% yield [22].



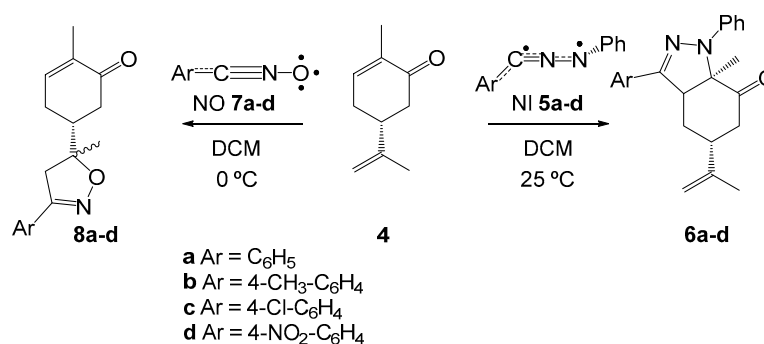
Scheme 3. Reactivity models associated to the four different TAC structures.



Scheme 4. Synthesis of spiro-isoxazoline derivatives of tomentosin **1**.

An MEDT study of this 32CA reaction accounted for the total chemo- and regioselectivity experimentally observed, emphasized the *zw-type* reactivity of the benzonitrile oxide **2**, and revealed that the reaction takes place through a non-concerted *two-stage one-step* mechanism [23] initialized with the formation of the C–C single bond involving the β -conjugated carbon of tomentosin **1**.

In 2019, Ait Itto et al. reported the 32CA reactions of (R)-carvone **4** with diaryl nitrilimines (NIs) **5a–d** and aryl nitrile oxides (NOs) **7a–d** in dichloromethane (DCM), yielding pyrazoles **6a–d** and isoxazoles **8a–d**, respectively (see Scheme 5) [24]. These 32CA reactions presented total regio- and chemoselectivity, obtaining a mixture of a pair of diastereoisomers resulting from the attack of these TACs by the two faces of the two C–C double bonds of (R)-carvone **4**. Interestingly, both regio- and chemoselectivity were opposite for the two TACs.



Scheme 5. 32CA reactions of (R)-carvone **4** with diaryl NIs **5a–d** and aryl-NOs **7a–d**.

An MEDT study of these 32CA reactions allowed explaining the different behaviours of these TACs [18]. The topological analysis of the ELF of diaryl NI **5a** and aryl NO **7a** allowed characterizing their electronic structure as carbenoid and zwitterionic TACs, respectively, thus presenting different *cb-* and *zw-type* reactivities, which were confirmed by an ELF topological analysis of the C–C, C–N and C–O single bond formation along the most favourable reaction path associated with these 32CA reactions. This MEDT study supported the classification of 32CA reactions into *pdr-*, *pmr-*, *cb-* and *zw-type*.

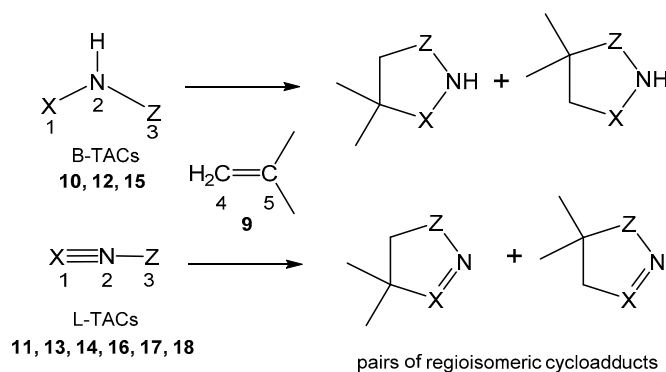
Organic reactions can also be classified as non-polar and polar reactions, in such a way that organic reactions are favoured with the increase of the polar character of the reaction [25]. In 2014, Domingo proposed the analysis of the global electron density transfer (GEDT) [26,27] at the transition state structures (TSs) as a measure of the polar character of a reaction. Reactions with GEDT values below 0.05 e correspond to non-polar processes, while values above 0.20 e correspond to polar processes. Very recently, organic reactions have been classified as forward electron density flux (FEDF) and reverse electron density flux (REDF) reactions, depending on the direction of the flux of the electron density at the TS [28]. Non-polar reactions are classified as null electron density flux (NEDF) reactions [29]. This classification is unequivocal, as the GEDT is a measure of the actual electron density transfer at the TSs. Thus, while the DA reaction between butadiene and ethylene was classified as “normal electron demand” [30] within Sustmann’s classification [31], it is classified as an NEDF reaction because of being non-polar; note that the GEDT at this DA reaction is negligible, 0.0 e [32].

Many TACs such as zwitterionic nitrones have nucleophilic character. Consequently, they react with strong electrophilic ethylenes, such as methyl acrylate or nitroethylene through a polar mechanism with high regioselectivity [33]. In these polar *zw-type* 32CA reactions, the analysis of the Parr functions allows explaining the observed regioselectivity. However, TACs as nitrile oxides, which participate in *zw-type* 32CA reactions with low polar character, show low reactivity and low regioselectivity [34]. In addition, many ethylene derivatives such as 2-methylpropene **9** do not have an electrophilic character, and consequently, the corresponding 32CA reactions have non-polar character. Note that many of the most common TACs neither have an electrophilic character as a consequence of the high electron density accumulation at the three centres of the TAC and, therefore, the corresponding reactions with nucleophilic ethylene derivatives will also have a low polar character.

Since non-polar 32CA reactions have not been studied as much as polar 32CA reactions, the 32CA cycloadditions of the nine simplest TACs **10** to **18** shown in Table 1 with 2-methylpropene **9** are herein studied within MEDT in order to understand the origin of the regioselectivity in non-polar 32CA reactions (see Scheme 6).

Table 1. Atom composition, name and structural classification of the nine TACs **10**–**18** studied herein.

	X1–N2–Z3	Name	Structure
10	H ₂ C–NH–CH ₂	azomethine ylide	bent
11	H ₂ C–N–CH	nitrile ylide	linear
12	H ₂ C–NH–NH	azomethine imine	bent
13	H ₂ C–N–N	diazomethane	linear
14	HC–N–NH	nitrile imine	linear
15	H ₂ C–NH–O	nitrone	bent
16	HC–N–O	nitrile oxide	linear
17	NH–N–N	azide	linear
18	N–N–O	nitrous oxide	linear



Scheme 6. Selected 32CA reactions of three bent, **10**, **12** and **15**, and six linear, **11**, **13**, **14**, **16**, **17** and **18**, simplest TACs with 2-methylpropene **9**.

2. Computational Methods

All stationary points were optimised using the B3LYP functional [35,36], together with the 6-311G(d,p) basis set [37]. This functional has been widely used in the study of 32CA reactions [38–41]. The optimisations were carried out using the Berny analytical gradient optimisation method [42,43]. The stationary points were characterized by frequency computations in order to verify that TSs have one and only one imaginary frequency. The intrinsic reaction coordinate (IRC) paths [44] were traced in gas phase in order to check and obtain the energy profiles connecting each TS to the two associated minima of the proposed mechanism, i.e., reactants and products, using the second order González–Schlegel integration method [45,46].

The electronic structures of the stationary points were characterized by Natural Population Analysis (NPA) [47,48] and by the topological analysis of the ELF [14]. CDFT reactivity indices [7,8] were computed at the B3LYP/6-31G(d) level as original reactivity scales were established at that method, using the equations given in reference 8. A non-published study of the electrophilicity and nucleophilicity indices of 25 single organic molecules computed using different DFT functionals and basis sets proved excellent linear correlations between them. The GEDT [18] was computed by the sum of the atomic charges (q) of the atoms belonging to each framework at the TSs; $GEDT = \sum q_i$.

All computations were carried out with the Gaussian 16 suite of programs [49]. ELF studies were performed with the TopMod program [50], using the corresponding B3LYP/6-311G(d,p) monodeterminantal wavefunctions and considering the standard cubical grid of step size of 0.1 Bohr. The molecular geometries and ELF basin attractor positions were visualised using the GaussView program [51], while the ELF localisation domains were represented with the Paraview software at an isovalue of 0.75 a.u. [52,53].

3. Results and Discussion

The present MEDT study has been divided into four parts: (i) in Section 3.1, a study of the electronic structure of the TACs through ELF topological and NPA analyses is performed; (ii) in Section 3.2, an analysis of the CDFT reactivity indices at the ground state (GS) of the reagents is carried out; (iii) in Section 3.3, a study of the reactivity and regioselectivity in the 32CA reactions of the nine TACs 10–18 with 2-methylpropene 9 is made; and finally, (iv) in Section 3.4, an ELF topological analysis of the more favourable regioisomeric TSs is carried out in order to understand the changes in electron density with respect to reagents, and thus, to understand the origin of regioselectivity.

3.1. ELF Topological Analysis of Reagents 9 to 18

ELF, first constructed by Becke and Edgecombe [14] and further developed by Silvi and Savin [54], permits the establishment of a straightforward quantitative connection between the electron density distribution and the chemical structure. A useful correlation between the electronic structure and the reactivity of the simplest TACs participating in 32CA reactions towards ethylene has been established [16]. Thus, the topological analysis of the ELF of the nine TACs 10–18 and 2-methylpropene 9 was performed in order to predict their reactivity in 32CA reactions [16]. The populations of the most significant valence basins are listed in Table 2, while the ELF basin attractor positions are shown in Figure 1. A picture of the ELF localisation domains of four representative TACs characterizing the four types of TACs, i.e., *pseudodiradical*, *pseudo(mono)radical*, carbenoid and zwitterionic, is shown in Figure 2. The ELF-based Lewis-like structures together with the natural atomic charges of the nine TACs are also shown in Figure 1.

At azomethine ylide 10, two pairs of monosynaptic basins, $V(C1)$ and $V'(C1)$, and $V(C3)$ and $V'(C3)$, integrating a total of 0.86 e each pair, are observed at the C1 and C3 carbon ends. These ELF $V(Ci)$ monosynaptic basins are related with the presence of two *pseudoradical* centers [55] at azomethine ylide 10, thus being considered as a *pseudodiradical* TAC. Note that *pseudoradical* centers in a tetrahedric

carbon are characterized by the presence of one V(C1) monosynaptic basin, while those in a trigonal planar carbon are usually characterized by the presence of two V(C1) and V'(C1) monosynaptic basins.

Table 2. Populations of the most significant ELF valence basins, in average number of electrons, e , of the nine TACs 10–18 and 2-methylpropene 9.

Basins	10	11	12	13	14	15	16	17	18	19
V(X1)	0.43	0.29	0.35	0.49	1.64			3.44	4.06	
V'(X1)	0.43	0.24	0.35	0.49						
V(X1,N2)	2.59	2.98	2.96	3.04	2.21	3.72	5.50	2.41	4.18	
V'(X1,N2)					2.27					
V(N2,Z3)	2.59	2.04	1.89	3.65	2.27	1.47	1.97	1.66	1.91	
V'(N2,Z3)		1.98						2.48		
V(Z3)	0.43	1.90	3.50	1.92	3.29	3.00	5.57	3.81	5.50	
V'(Z3)	0.43			1.92		2.84				
V(C4,C5)										1.76
V'(C4,C5)										1.76

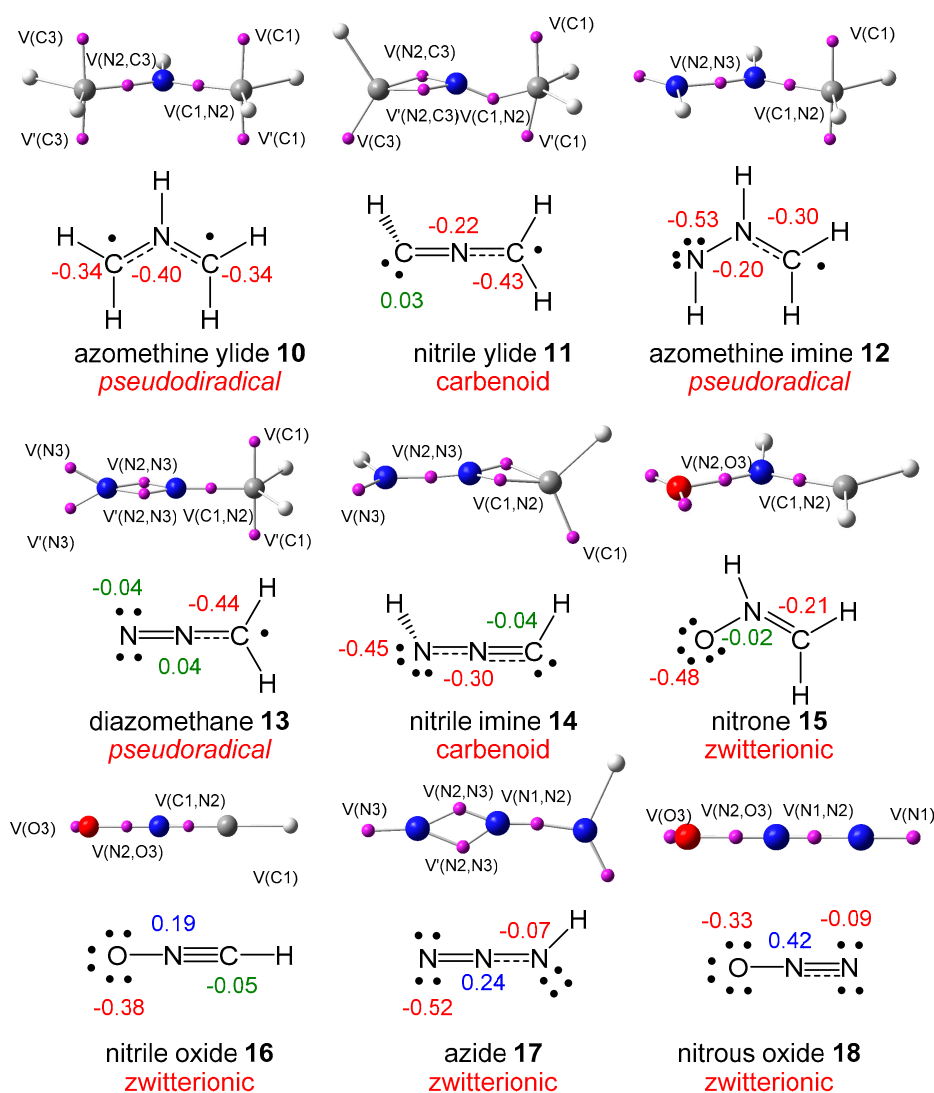


Figure 1. ELF basin attractor positions, ELF-based Lewis-like structures and TAC classifications, together with calculated natural atomic charges, in average number of electrons e , of TACs 10–18. Negative charges are coloured in red, positive charges in blue, and negligible charges in green.

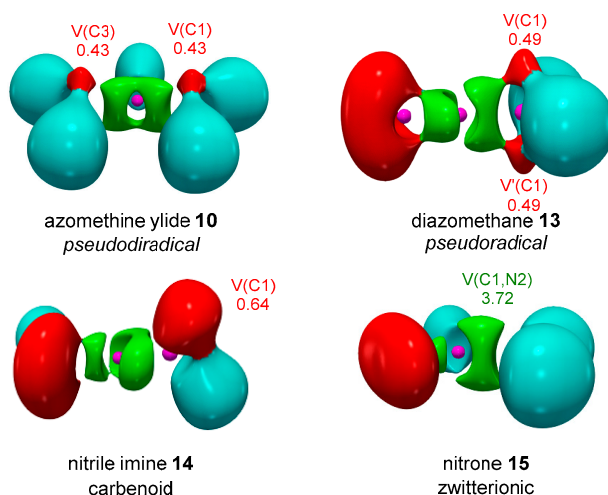


Figure 2. B3LYP/6-311G(d,p) ELF localisation domains represented at an isosurface value of ELF = 0.75, together with the populations, given in average number of electrons, *e*, of the valence basins characterizing the type of TAC for azomethine ylide **10**, *pseudodiradical*, diazomethane **13**, *pseudo(mono)radical*, nitrile imine **14**, carbenoid, and nitron **15**, zwitterionic. V(X1,N2) and V(N2,Z3) disynaptic basins are represented in green, V(C,H) and V(N2,H) protonated basins are represented in turquoise, V(C), V(N) and V(O) monosynaptic basins are represented in red, and C(C), C(N) and C(O) core basins are represented in pink.

At azomethine imine **12** and diazoalkane **13**, two pairs of monosynaptic basins, V(C1) and V'(C1), integrating a total of 0.60 *e* and 0.98 *e*, respectively, are observed at the trigonal planar C1 carbon. For these TACs, these V(C1) monosynaptic basins are related with the presence of one *pseudoradical* center at the C1 carbon of these TACs, thus being considered as *pseudoradical* TACs.

At nitrile ylide **11** and nitrile imine **14**, one single V(Ci) monosynaptic basin, integrating 1.90 *e* (**11**) and 1.64 *e* (**14**), is observed at the C3 and C1 carbon, respectively, being associated to one carbenoid center, both being thus considered as carbenoid TACs. Note that nitrile ylide **11** also presents two monosynaptic basins, V(C1) and V'(C1), with a total low population of 0.53 *e*, at the C1 carbon (see Table 2), being associated with a *pseudoradical* center.

Neither *pseudoradical* nor carbenoid centres appear in TACs **15**–**18**, but there are disynaptic basins, V(X1,N2), V'(X1,N2), V(N2,Z3) and V'(N2,Z3), whose populations are associated to multiple bonds, thus being considered as zwitterionic TACs [16]. The V(Z3) monosynaptic basins present at these TACs, which are associated to C, N or O non-bonding electron density regions, correspond with the lone pairs of the Lewis-like structures (see Figure 1).

On the other side, the population of the V(X1,N2) and V(N2,Z3) disynaptic basins associated to the L-TACs indicates that, except nitrile imine **14**, nitrile oxide **16** and nitrous oxide **18**, which have a propargylic structure, X1≡N2–Z3, the other TACs have a rather allenic structure, X1=N2=Z3.

Finally, 2-methylpropene **9** shows the presence of a pair of disynaptic basins, V(C4,C5) and V'(C4,C5), with a total population of 3.52 *e*, respectively, being associated to an underpopulated C4–C5 double bond.

ELF topological analysis of the nine TACs **10**–**18** shows that while some zwitterionic TACs such as nitron **6** correspond with Huisgen's 1,2-dipolar structure [56], *pseudodiradical* and *pseudo(mono)radical* TACs, such as azomethine ylide **10** and diazomethane **13**, correspond with Firestone's radical structures [57]. However, it is interesting to remark that while *pseudodiradical* and *pseudo(mono)radical* TACs are species with a stable closed-shell electronic structure [55], actual radical species have open-shell electronic structures.

NPA analysis of the natural atomic charges at the nine TACs **10**–**18** shows that, except for nitrile oxide **16**, azide **17** and nitrous oxide **18**, all TACs has a rather negatively charged framework (see Figure 2), thus ruling out the commonly accepted charge distribution of a 1,2-zwitterionic Lewis

structure [16]. These atomic charge distributions result from the more electronegative character of the C, N and O atoms than the H atoms bound to them. Consequently, the atomic charge distribution on the TACs does not come from resonant electronic structures, but from the anisotropic distribution of the electron density generated by the different nuclei belonging to the TAC [16].

3.2. Analysis of the Global and Local CDFT Reactivity Indices at the GS of the Reagents

The analysis of the reactivity indices based on CDFT has become a useful tool for the study of reactivity in polar reactions [8]. Therefore, in order to establish the polar or non-polar character of these 32CA reactions, an analysis of CDFT reactivity indices was performed. The CDFT indices were calculated at the B3LYP/6-31G(d) computational level since it was used to define the electrophilicity and nucleophilicity scales [8]. The B3LYP/6-31G(d) global indices, namely, the electronic chemical potential, μ , chemical hardness, η , electrophilicity, ω , and nucleophilicity, N , at the GS of TACs **10** to **18** and 2-methylpropene **9**, are given in Table 3.

Table 3. B3LYP/6-31G(d) global CDFT indices, namely, the electronic chemical potential μ , the chemical hardness η , and the electrophilicity ω and nucleophilicity N indices, in eV, at the GS of TACs **10** to **18** and 2-methylpropene **9**.

Reagent	μ	η	ω	N
10	-1.82	4.47	0.37	5.07
11	-2.90	5.45	0.77	3.50
12	-2.70	5.02	0.72	3.92
13	-3.64	4.73	1.40	3.11
14	-3.55	5.87	1.07	2.64
15	-3.43	5.55	1.06	2.92
16	-3.40	7.97	0.73	1.75
17	-4.24	6.54	1.37	1.62
18	-4.92	8.79	1.37	-0.19
9	-2.83	7.37	0.55	2.60

The electronic chemical potential [7] μ of the nine TACs ranges from -1.81 (**10**) to -4.92 (**18**) eV, while that of 2-methylpropene **9** is -2.83 eV. Except for TACs **10–12**, TACs **13–18** have lower chemical potential than 2-methylpropene **9**, suggesting that the electron density will flux from 2-methylpropene **9** towards those TACs. On the other hand, in general, the hardness [58] η of these TACs increases along this series of TACs. Thus, while azomethyne ylide **10** has a $\eta = 4.47$ eV, azide **18** has a $\eta = 8.79$ eV. Thus, azomethyne ylide **10** is the softest TAC, while azide **18** is the hardest TAC.

The electrophilicity ω index [9] of these TACs ranges from 0.37 (**10**) to 1.37 (**18**) eV. Thus, while TACs **10**, **11**, **12** and **16** are classified as marginal electrophiles, TACs **13**, **14**, **15**, **17** and **18** are classified as moderate electrophiles within the electrophilicity scale [8]. On the other hand, while the nucleophilicity N index [10] for TACs **10**, **11**, **12** and **13** is higher than 3.0 eV, being classified as strong nucleophiles, TACs **11**, **14**, and **15** are classified as moderate nucleophiles, and TACs **16** to **18**, having a nucleophilicity N index lower than 2.0 eV, are classified as marginal nucleophiles within the nucleophilicity scale [8]. The high nucleophilicity N index of azomethyne ylide **10** permits its classification as a supernucleophile [59].

The electrophilicity ω and nucleophilicity N indices of 2-methylpropene **9** are 0.55 and 2.60 eV, respectively, being classified as a marginal electrophile and a moderate nucleophile. Thus, while 2-methylpropene **9** will never participate as electrophile in polar reactions, it could participate as nucleophile only towards strong electrophilic species, which is not the case.

As the polar character of organic reactions is mainly controlled by electrophilic species, the low electrophilic character of these species suggests that the corresponding 32CA reactions will have low polar character.

Along a polar reaction involving the participation of non-symmetric reagents, the most favourable reactive channel is that involving the initial two-centre interaction between the most electrophilic

centre of the electrophile and the most nucleophilic centre of the nucleophile [6]. In this context, the electrophilic P_k^+ and nucleophilic P_k^- Parr functions [11] derived from the excess of spin electron density reached via the GEDT [26] process from the nucleophile toward the electrophile have shown to be one of the most accurate and insightful tools for the study of the local reactivity in polar and ionic processes. Although the 32CA reaction under study will have a low polar character, the electrophilic P_k^+ and nucleophilic P_k^- Parr functions of three selected TACs, a *pseudoradical*, diazomethane **13**, a carbenoid, nitrile imine **14**, and a zwitterionic, nitron **15**, as well as 2-methylpropene **9**, were analysed in order to characterize what would be the corresponding regioselectivity in polar 32CA reactions (see Figure 3).

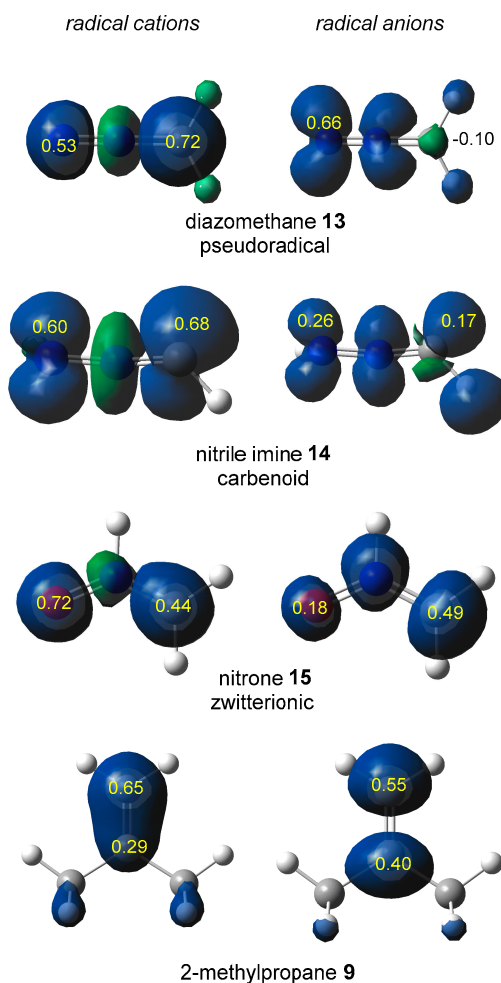


Figure 3. 3D representations of the Mulliken atomic spin densities of the radical cation and radical anion of diazomethane **13**, nitrile imine **14**, nitron **15**, and 2-methylpropene **9**, together with the nucleophilic P_k^- (left side) and electrophilic P_k^+ (right side) Parr functions.

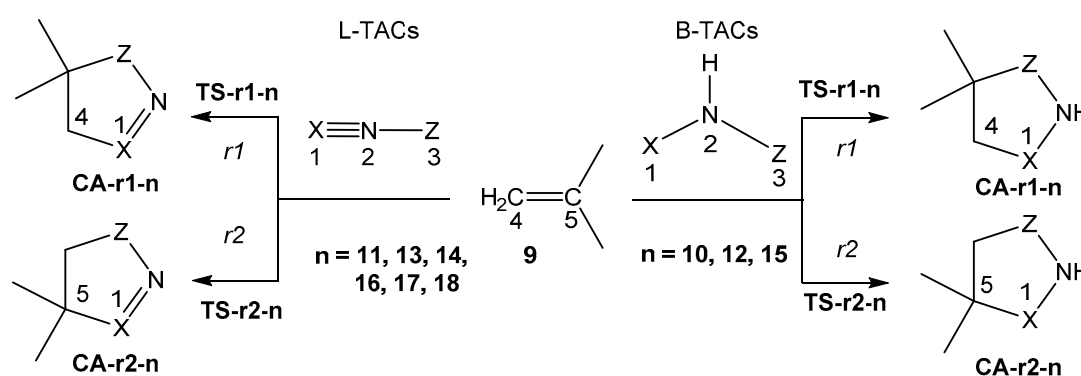
Electrophilic and nucleophilic substituted ethylenes have the most electrophilic and nucleophilic centers at the non-substituted CH_2 methylene carbon of the ethylene [33]; see the electrophilic P_k^+ and nucleophilic P_k^- Parr functions of 2-methylpropene **9** in Figure 3. Analysis of the electrophilic P_k^+ and nucleophilic P_k^- Parr functions of the three selected TACs shows that along polar 32CA reactions, a change in regioselectivity will be expected depending on whether the reaction is classified as FEDF or REDF [28]. As many of the TACs are more nucleophilic than electrophilic, see Table 3, analysis of the nucleophilic P_k^- Parr functions will permit to predict the regioselectivity in a FEDF 32CA reaction.

Interestingly, in 32CA reactions of FEDF, zwitterionic nitron **16** shows a reverse regioselectivity than *pseudoradical* diazomethane **13** and carbenoid nitrile imine **14**. Thus, while diazomethane **13** and

nitrile imine **14** present the most nucleophilic center at the *pseudoradical* and carbenoid C1 carbons, nitron **15** presents the most nucleophilic center at the O3 oxygen.

3.3. Study of the Reactivity and Regioselectivity in the 32CA Reactions of TACs **10–18** with 2-Methylpropene **9**

Except for azomethine ylide **10**, the rest of the reagents do not present molecular symmetry; thus, eight of the selected 32CA reactions can occur through two competitive regioisomeric reaction paths; the first ones, denoted as *r1*, are related to the formation of the X1–C4 single bond, while the second ones, denoted as *r2*, are associated to the formation of the Z3–C4 bond (see Scheme 7). Searching for the stationary points along each of the two regioisomeric reaction paths revealed only one TS and its corresponding cycloadduct; thus, these 32CA reactions are meant to occur through a one-step mechanism. Relative energies of the stationary points involved in the nine 32CA reactions are given in Table 4.



Scheme 7. Regioisomeric reaction paths associated to the 32CA reactions of TACs **10–18** with 2-methylpropene **9**.

Table 4. Relative electronic energies, ΔE , in kcal·mol⁻¹, of the TSs and cycloadducts involved in the 32CA reactions of TACs **10** to **18** with 2-methylpropene **9**.

TAC	type	TS-r1-n	TS-r2-n	CA-r1-n	CA-r2-n
10	<i>pdr</i>	8.8		-54.6	
11	<i>cb</i>	14.0	15.0	-59.5	-59.4
12	<i>pmr</i>	12.8	15.3	-39.7	-36.7
13	<i>pmr</i>	20.4	23.1	-23.1	-27.0
14	<i>cb</i>	11.8	14.4	-54.0	-51.3
15	<i>zw</i>	14.4	19.8	-27.1	-22.0
16	<i>zw</i>	15.0	19.9	-38.3	-32.7
17	<i>zw</i>	23.7	23.1	-17.3	-16.7
18	<i>zw</i>	27.7	30.5	-2.9	-1.3

The activation energies associated to the nine 32CA reactions range from 8.8 (**10**) to 27.7 (**18**) kcal·mol⁻¹, the reactions being exothermic by between 2.9 (**18**) and 59.5 (**11**) kcal·mol⁻¹. Some appealing conclusions can be drawn from the relative energies given in Table 4: (i) the most favourable 32CA reaction corresponds to that involving *pseudodiradical* azomethyne ylide **10**, $\Delta E_{\text{act}} = 8.8$ kcal·mol⁻¹, while the most unfavourable one corresponds to that involving zwitterionic nitrous oxide **18**, $\Delta E_{\text{act}} = 27.7$ kcal·mol⁻¹; (ii) except for diazomethane **13**, the general trend of reactivity *pdr-type* > *pmr-type* ≥ *cb-type* > *zw-type* is observed [16]; (iii) except for the 32CA reaction involving azide **17**, which is slightly *r2* regioselective [33], seven of these 32CA reactions are *r1* regioselective. Note that in the case of nitron **6**, the *r1* regioselectivity is opposite to that observed in polar *zw-type* 32CA reactions involving electrophilic ethylenes [32]; (iv) the regioselectivity, measured as $\Delta\Delta E_{\text{act}}$, ranges from 1.0 kcal·mol⁻¹ for the 32CA reaction involving nitrile ylide **11** to 5.3 kcal·mol⁻¹ for the 32CA reaction

involving nitrene **15**; excluding TACs **10**, **11** and **17**, the other four 32CA reactions can be considered highly *r1* regioselective with $\Delta\Delta E_{\text{act}} > 2.5 \text{ kcal}\cdot\text{mol}^{-1}$; (v) considering the strong exothermic character of the 32CA reactions of TACs **10–16**, $\Delta E_{\text{reac}} > 22.3 \text{ kcal}\cdot\text{mol}^{-1}$, these reactions can be considered irreversible, and consequently, formation of the *r1* regioisomeric cycloadducts is kinetically controlled; and (vi) in general, except for diazomethane **13**, all *r1* regioisomeric cycloadducts are thermodynamically more stable than the *r2* ones. Consequently, except for the reactions involving TACs **13** and **17**, the *r1* regioisomeric cycloadducts can also be considered the thermodynamic control product.

Considering that in the series of TACs **11–18** the X1 end atom is less electronegative than the Z3 one, i.e., the electronegativity increases in the order $\text{C} < \text{N} < \text{O}$, and the trigonal planar arrangement is less electronegative than the linear one, it is possible to conclude that the *r1* regioselectivity observed in these 32CA reactions is kinetically controlled by the interactions between the least electronegative X1 end atom of these TACs and the methylene C4 carbon of 2-methylpropene **9**.

The optimized geometries of the most favourable *r1* regioisomeric TSs are shown in Figure 4, while the distances between C–C, C–N and C–O interacting centers at the two regioisomeric TSs are given in Table 5. Some appealing conclusions can be drawn from these geometrical parameters: (i) the distance between the interacting centres at the *r1* regioisomeric TSs ranges from 2.442 Å (C–C) at **TS-r1-10** to 1.995 Å (C–N) at **TS-r1-18**; (ii) the C4–X1 (X=C, N, O) distances decrease with the increase of the activation energy; i.e., the more unfavourable the TS, the more advanced it is; (iii) considering that the formation of the C–C, C–N and C–O single bonds begins in the short ranges of 2.00–1.90, 1.90–1.80 and 1.80–1.70 Å [16], respectively, these distances indicate that the formation of the C4–X1 (C, N, O) new single bonds has not started yet at any TS (see Section 3.4); and, finally (iv) except for **TS-r1-11**, the distance involving the X1 end atom of these TACs is shorter than that involving the Z3 one. These behaviours point out that the interaction between the least electronegative X1 atom of these TACs and the methylene C4 carbon of **9** is less unfavourable and more advanced than that involving the more electronegative Z3 atom.

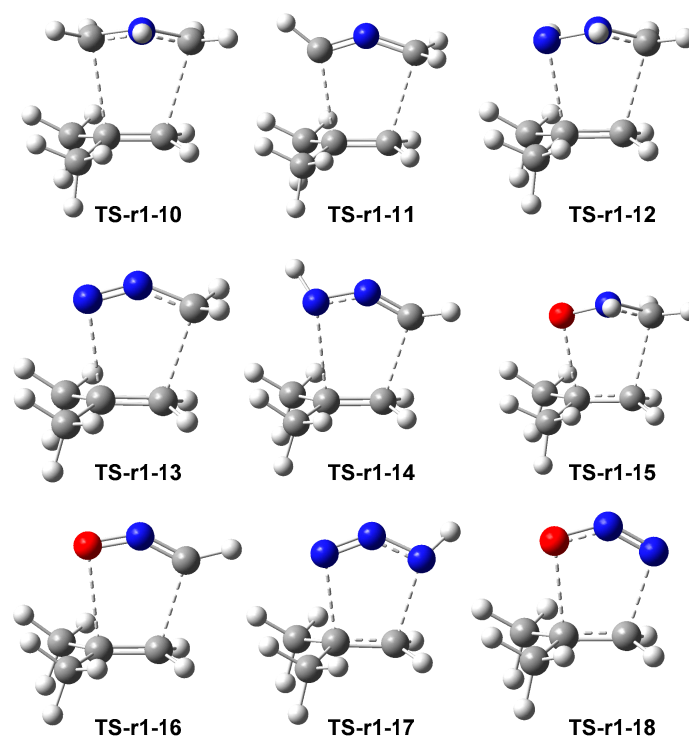


Figure 4. Geometries of the most favourable *r1* regioisomeric TSs involved in the 32CA reactions of TACs **10** to **18** with 2-methylpropene **9**.

Table 5. Cx-Xy (X=C, N, O) distances, in angstroms Å, at the r1 and r2 regioisomeric TSs involved in the 32CA reactions of TACs **10** to **18** with 2-methylpropene **9**.

TAC	TS-r1-n		TS-r2-n	
	C4-X1	C5-X3	C4-X3	C5-X1
10	2.442	2.445		
11	2.423	2.415	2.471	2.374
12	2.266	2.319	2.308	2.239
13	2.234	2.324	2.280	2.228
14	2.222	2.534	2.392	2.276
15	2.174	2.213	2.140	2.160
16	2.192	2.483	2.352	2.182
17	2.131	2.140	2.054	2.189
18	1.995	2.176	2.083	2.028

In order to evaluate the polar nature of these 32CA reactions, the GEDT [18] at the TSs was analysed. Reactions with GEDT values below 0.05 e correspond to non-polar processes, while values above 0.20 e correspond to polar processes. The GEDT values measured at the TAC framework of the more favourable r1 regioisomeric TSs are 0.14 e at **TS-r1-10**, −0.09 e at **TS-r1-11**, 0.07 e at **TS-r1-12**, 0.07 e at **TS-r1-13**, −0.03 e at **TS-r1-14**, −0.01 e at **TS-r1-15**, −0.05 e at **TS-r1-16**, −0.08 e **TS-r1-17** and −0.19 e at **TS-r1-18**. Some appealing conclusions can be drawn from these GEDT values: (i) while the 32CA reactions of azomethine ylide **10** and nitrous oxide **18** have polar character, those of TACs **11–17** have a low-polar or non-polar character; (ii) while the 32CA reaction of azomethine ylide **10** is classified as FEDF, that of nitrous oxide **18** is classified as REDF [28]. Note the change of the sign of the GEDT at **TS-r1-10**, 0.14 e, and at **TS-r1-18**, −0.19 e; thus, while azomethine ylide **10** acts as electron-donor, nitrous oxide **18** acts as electron-acceptor. This is a consequence of the supernucleophilic character [59] of **10** and the moderate electrophilic character of **18** (see Table 3); and finally, (iii) the non-polar 32CA reactions of nitrile imine **14** and nitrene **15** can be classified as NEDF [29].

3.4. ELF Topological Analysis of the Most Favourable r1 Regioisomeric TSs

Finally, the electronic structure of the more favourable r1 regioisomeric TSs was analysed through a topological analysis of the ELF. The ELF valence basin populations of the nine TSs are given in Table 6, while a picture of the ELF basin attractor positions of the TSs is shown in Figure 5.

Analysis of the basin populations of the nine TSs shows that they present great similitudes. All TSs show a V(N2) monosynaptic basin, with a population ranging from 0.73 e (**TS-r1-10**) to 2.33 e (**TS-r1-18**). In general, the population of this V(N2) monosynaptic basin increases with the advanced character of the TS. Thus, its population, which mainly comes from the depopulation of the X1–N2 bonding region of the TACs, reaches the maximum value at the final cycloadducts. This V(N2) monosynaptic basin, which is not present at the TACs (see Table 2), is associated to the N2 non-bonding electron density present at the final cycloadduct.

All C1 and C3 end carbons present one or two V(C) monosynaptic basins, integrating between 0.51 e (**TS-r1-10**) and 1.47 e (**TS-r1-18**). Interestingly, while these V(C) monosynaptic basins are already present at the *pseudoradical* and carbenoid TACs, they must be created at the zwitterionic TACs such as nitrene **15** and nitrile oxide **16** by depopulation of the C–N2 bonding region. This behaviour, together with the creation of the V(N2) monosynaptic basin, accounts for the higher activation energies of the TSs associated to *zw-type* 32CA reactions [16]. Note that these V(Ci) monosynaptic basins are demanded for the subsequent C–C single bond formation [26].

Except for the unfavourable **TS-r1-18**, the N and O centres show the presence of V(N) or V(O) monosynaptic basins, associated to N or O non-bonding electron density, which are already present at the corresponding TACs. Note that the formation of the subsequent N–C or O–C single bonds results

from the participation of part of the non-bonding electron density of the N or O atoms and that of the *pseudoradical* carbon of the ethylene derivative.

Finally, ELF of the ethylene framework shows the presence of one V(C4,C5) disynaptic basin, integrating between 3.06 e (TS-r1-18) and 3.41 e ((TS-r1-10). Note that the population of the V(C4,C5) disynaptic basin at 2-methylpropene **9** is 3.52 e. Along the reaction path, ongoing from the separated reagents to TSs, the C–C bonding region of 2-methylpropene **9** is depopulated in order to generate, after passing the TSs, the V(C4) and V(C5) monosynaptic basins required for the formation of the new X–C single bonds. As a consequence of this continue depopulation, the two V(C4,C5) and V'(C4,C5) disynaptic basins present at 2-methylpropene **9** have merged into one single V(C4,C5) disynaptic basin at the nine TSs.

Table 6. ELF valence basin populations of the TSs associated to the *r1* regioisomeric reaction path of the 32CA reactions of TACs **10** to **18** with 2-methylpropene **9**, in average number of electrons, e.

Basins	TS-r1-10	TS-r1-11	TS-r1-12	TS-r1-13	TS-r1-14	TS-r1-15	TS-r1-16	TS-r1-17	TS-r1-18
V(X1)	0.63	0.51	0.59	0.91	0.44	1.47	1.33	3.38	3.84
V(X1,N2)	2.32	2.24	2.31	1.92	2.39	2.93	1.55	2.71	2.72
V'(X1,N2)						1.55			
V(N2)	0.73	1.54	1.12	1.97	1.32	2.09	2.04	2.26	2.33
V(N2,Z3)	2.30	1.67	1.71	1.55	1.24	1.88	1.49	2.71	1.44
V'(N2,Z3)		1.67		1.43					
V(Z3)	0.73	1.63	3.35	3.75	2.86	3.32	2.82	3.87	5.22
V'(Z3)					2.99		2.82		0.40
V(C4,C5)	3.41	3.30	3.35	3.31	3.25	3.23	3.20	3.14	3.06

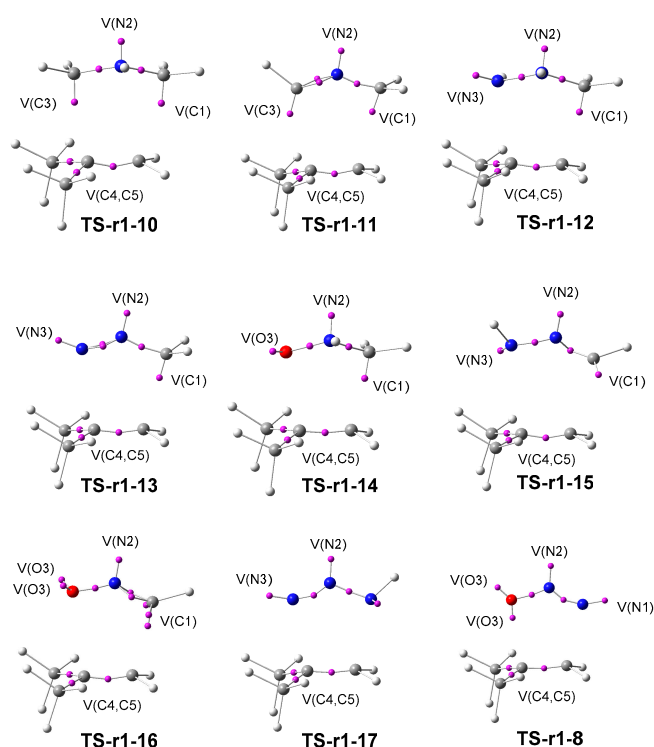


Figure 5. ELF basin attractor positions of the TSs associated to the *r1* regioisomeric reaction path of the 32CA reactions of TACs **10** to **18** with 2-methylpropene **9**.

From the ELF topological analysis of the nine TSs, one relevant conclusion can be drawn. Even despite the different behaviour of the C, N and O end centres, the nine TSs present a similar electronic structure [16]; all end carbons of the TACs have one V(C1) monosynaptic basin associated to a *pseudoradical* or carbene centre, while the nitrogen and oxygen end centres have V(N) or V(O) monosynaptic basins associated to N or O non-bonding electron density. Only changes in the population of these V(X) monosynaptic basins with the advanced character of the TSs are found. On the other

hand, the C4–C5 double bond region of the ethylene framework shows a depopulation, which also increases with the advanced character of the TS. However, neither V(C4) nor V(C5) monosynaptic basin is observed in the ethylene framework at the nine TSs.

As the activation energies associated to these non-polar 32CA reactions are mainly associated to the depopulation of the N2–X1 and C4–C5 bonds, which is required for the formation of the non-bonding electron density demanded for the single bond formation, i.e., the *pseudoradical* centres at carbon atoms [26], the different activation energies found in these 32CA reactions depend on the presence of the V(X1) (X=C, N, O) monosynaptic basins at the corresponding TACs, thus justifying the order of reactivity *pseudodiradical* > *pseudoradical* ≥ carbenoid > zwitterionic.

Finally, the V(C1) monosynaptic basins present at the TSs, which are associated with a *pseudoradical* or carbenoid center required for the subsequent C1–C4 single bond formation, appear, or are already present at the TAC, at the least electronegative end carbon atom of these TACs. As these V(C1) monosynaptic basins are created by the depopulation of the neighboring C1–N2 bonding region in zwitterionic TACs, they demand a higher energy cost. On the other hand, in TACs in which the formation of the X1–C4 single bond involves the participation of a nitrogen or oxygen atom, formation of these X1–C4 single bonds demands the donation of part of the non-bonding electron density of these heteroatoms. Consequently, it is reasonable to understand that the changes in electron density required for the formation of the new X1–C4 single bonds will take place more easily at the end centre involving the least electronegative X1 atom. This interpretation accounts for the regioselectivity found in these non-polar 32CA reactions.

4. Conclusions

The 32CA reactions of nine simplest TACs 10–18 with 2-methylpropene 9 have been studied within MEDT at the MPWB1K/6-311G(d,p) computational level in order to understand the origin of the regioselectivity in non-polar 32CA reactions.

Topological analysis of the nine simplest TACs 10–18 allows their classification into one of the four types of TACs: *pseudodiradical*, *pseudo(mono)radical*, carbenoid and zwitterionic ones. On the other hand, the NPA shows that many of the atoms of these TACs are negatively charged, thus ruling out the commonly accepted charge distribution of a 1,2-zwitterionic Lewis structure.

CDFT classifies TACs 1, 2, 3 and 7 as marginal electrophiles, and TACs 13, 14, 15, 17 and 18 as moderate electrophiles. On the other hand, TACs 10, 12 and 13 are classified as strong nucleophiles, TACs 11, 14 and 15 as moderate nucleophiles, and TACs 16 to 18 as marginal nucleophiles. Consequently, only TACs 10, 12 and 13 will participate as strong nucleophiles in polar 32CA reactions of FEDF.

The activation energies associated to the nine 32CA reactions range from 8.8 (10) to 27.7 (18) kcal·mol⁻¹, the reactions being exothermic by between 2.9 (18) and 59.5 (11) kcal·mol⁻¹. The general trend of reactivity, *pdr-type* > *pmd-type* ≥ *cb-type* > *zw-type*, is observed in this series of 32CA reactions. Except for the 32CA reaction involving azide 17, which is slightly *r2* regioselective, all these 32CA reactions are *r1* regioselective.

Analysis of the geometries of the more favourable *r1* regioisomeric TSs indicates that the distance between the interacting centres ranges from 2.442 (C–C) Å at TS-r1-10 to 1.995 (C–N) at TS-r1-18. The C–X (X=C, N, O) distances decrease with the increase of the activation energy, i.e., the more unfavourable the TS, the more advanced it is. Except for TS-r1-11, the distance involving the X1 end atom of these TACs is shorter than that involving the Z3 one. These behaviours point out that in these non-polar 32CA reactions, the interactions between the least electronegative X1 atom of these TACs and the methylene C4 carbon of 9 are less unfavourable and more advanced than those involving the most electronegative Z3 atom.

The computed GEDT values at the more favourable *r1* regioisomeric TSs indicate that while the 32CA reactions of TACs 10 and 18 have polar character, those of TACs 11–17 have a low-polar or non-polar character.

A comparative analysis of the topology of the ELF of the more favourable *r1* regioisomeric TSs shows that they present a similar electronic structure. As the X1–C4 bond formation requires X1 non-bonding electron density, the different activation energies observed in these 32CA reactions mainly depend on the presence of V(X1) monosynaptic basins at the TACs and the energy cost associated to the depopulation of the N2–X1 and C4–C5 bonds, thus justifying the order of reactivity *pseudodiradical* > *pseudoradical* > carbenoid > zwitterionic.

From this MEDT study it is possible to conclude that the lesser energetic cost demanded for the creation of the non-bonding electron density at the least electronegative X1 atom of these TACs, which is required for the subsequent X1–C4 single bond formation, is responsible for the regioselectivity of these low polar 32CA reactions.

Author Contributions: L.R.D. headed the subject, wrote the manuscript and performed calculations; M.R.G. headed the subject, performed calculations and wrote the manuscript; and J.C.S. performed calculations and wrote the manuscript. All authors have read and agreed to the published version of the manuscript.

Funding: This research was funded by the Ministry of Science and Innovation (MICINN) of the Spanish Government, project PID2019-110776GB-I00 (AEI/FEDER, UE), and European Union's Horizon 2020 research and innovation programme under the Marie Skłodowska-Curie, grant agreement No. 846181.

Conflicts of Interest: There are no conflict to declare.

References

1. Moss, G.P.; Smith, P.A.S.; Tavernier, D. Glossary of class names of organic compounds and reactivity intermediates based on structure (IUPAC Recommendations 1995). *Pure Appl. Chem.* **1995**, *67*, 1307–1375. [[CrossRef](#)]
2. Carruthers, W. *Some Modern Methods of Organic Synthesis*, 2nd ed.; Cambridge University Press: Cambridge, UK, 1978.
3. Carruthers, W. *Cycloaddition Reactions in Organic Synthesis*; Pergamon: Oxford, UK, 1990.
4. Padwa, A. *1,3-Dipolar Cycloaddition Chemistry*; Wiley-Interscience: New York, NY, USA, 1984; Volume 1–2.
5. Domingo, L.R.; Aurell, M.J.; Pérez, P.; Contreras, R. Quantitative characterization of the local electrophilicity of organic molecules. Understanding the regioselectivity on Diels-Alder reactions. *J. Phys. Chem. A* **2002**, *106*, 6871–6875. [[CrossRef](#)]
6. Aurell, M.J.; Domingo, L.R.; Pérez, P.; Contreras, R. A theoretical study on the regioselectivity of 1,3-dipolar cycloadditions using DFT-based reactivity indexes. *Tetrahedron* **2004**, *60*, 11503–11509. [[CrossRef](#)]
7. Parr, R.G.; Yang, W. *Density Functional Theory of Atoms and Molecules*; Oxford University Press: New York, NY, USA, 1989.
8. Domingo, L.R.; Ríos-Gutiérrez, M.; Pérez, P. Applications of the conceptual density functional indices to organic chemistry reactivity. *Molecules* **2016**, *21*, 748. [[CrossRef](#)] [[PubMed](#)]
9. Parr, R.G.; Szentpaly, L.v.; Liu, S. Electrophilicity index. *J. Am. Chem. Soc.* **1999**, *121*, 1922–1924. [[CrossRef](#)]
10. Domingo, L.R.; Chamorro, E.; Pérez, P. Understanding the reactivity of captodative ethylenes in polar cycloaddition reactions. A theoretical study. *J. Org. Chem.* **2008**, *73*, 4615–4624. [[CrossRef](#)] [[PubMed](#)]
11. Domingo, L.R.; Pérez, P.; Sáez, J.A. Understanding the local reactivity in polar organic reactions through electrophilic and nucleophilic Parr functions. *RSC Adv.* **2013**, *3*, 1486–1494. [[CrossRef](#)]
12. Domingo, L.R. Molecular electron density theory: A modern view of reactivity in organic chemistry. *Molecules* **2016**, *21*, 1319. [[CrossRef](#)]
13. Fukui, K. *Molecular Orbitals in Chemistry, Physics, and Biology*; Academic Press: New York, NY, USA, 1964.
14. Becke, A.D.; Edgecombe, K.E. A simple measure of electron localization in atomic and molecular-systems. *J. Chem. Phys.* **1990**, *92*, 5397–5403. [[CrossRef](#)]
15. Bader, R.F.W. *Atoms in Molecules: A Quantum Theory*; Clarendon Press: Oxford, UK, 1994.
16. Ríos-Gutiérrez, M.; Domingo, L.R. Unravelling the mysteries of the [3+2] cycloaddition reactions. *Eur. J. Org. Chem.* **2019**, 267–282. [[CrossRef](#)]
17. Zeroual, A.; Ríos-Gutiérrez, M.; El Idrissi, M.; El Alaoui El Abdallaoui, H.; Domingo, L.R. An MEDT Study of the Mechanism and Selectivities of the [3+2] Cycloaddition Reaction of Tomentosin with Benzonitrile Oxide. *Int. J. Quantum Chem.* **2019**, *119*, e25980. [[CrossRef](#)]

18. Ríos-Gutiérrez, M.; Domingo, L.R.; Esseffar, M.; Oubella, A.; Ait Itto, M.Y. Unveiling the Different Chemical Reactivity of Diphenyl Nitrilimine and Phenyl Nitrile Oxide in [3+2] Cycloaddition Reactions with (R)-Carvone through the Molecular Electron Density Theory. *Molecules* **2020**, *25*, 1085. [[CrossRef](#)]
19. Domingo, L.R.; Ríos-Gutiérrez, M.; Acharje, N. A Molecular Electron Density Theory Study of the Chemoselectivity, Regioselectivity and Diastereofacial Selectivity in the Synthesis of an Anti-Cancer Spiroisoxazoline derived from α -Santonin. *Molecules* **2019**, *24*, 832. [[CrossRef](#)] [[PubMed](#)]
20. Domingo, L.R.; Ghodsi, F.; Ríos-Gutiérrez, M. A Molecular Electron Density Theory Study of the Synthesis of Spirobipyrazolines through the Domino Reaction of Nitrilimines with Allenates. *Molecules* **2019**, *24*, 4159. [[CrossRef](#)]
21. Rhyman, L.; Ríos-Gutiérrez, M.; Domingo, L.R.; Ramasami, P. Unveiling the High Reactivity of Benzyne in the Formal [3+2] Cycloaddition Reactions towards Thioamides through the Molecular Electron Density Theory. *Tetrahedron* **2020**, *76*, 131458. [[CrossRef](#)]
22. Zaki, M.; Oukhrib, A.; Akssira, M.; Berteina-Raboin, S. Synthesis of novel spiro-isoxazoline and spiroisoxazolidine derivatives of tomentosin. *RSC Adv.* **2017**, *7*, 6523–6529. [[CrossRef](#)]
23. Domingo, L.R.; Sáez, J.A.; Zaragoza, R.J.; Arnó, M. Understanding the Participation of Quadricyclane as Nucleophile in Polar $[2\sigma + 2\sigma + 2\pi]$ Cycloadditions toward Electrophilic π Molecules. *J. Org. Chem.* **2008**, *73*, 8791–8799. [[CrossRef](#)]
24. Oubella, A.; Ait Itto, M.Y.; Auhmani, A.; Riahi, A.; Robert, A.; Daran, J.-C.; Morjani, H.; Parish, C.A.; Esseffar, M. Diastereoselective synthesis and cytotoxic evaluation of new isoxazoles and pyrazoles with monoterpenic skeleton. *J. Mol. Struct.* **2019**, *1198*, 126924. [[CrossRef](#)]
25. Domingo, L.R.; Sáez, J.A. Understanding the mechanism of polar Diels–Alder reactions. *Org. Biomol. Chem.* **2009**, *7*, 3576–3583. [[CrossRef](#)]
26. Domingo, L.R. A new C-C bond formation model based on the quantum chemical topology of electron density. *RSC Adv.* **2014**, *4*, 32415–32428. [[CrossRef](#)]
27. Domingo, L.R.; Ríos-Gutiérrez, M.; Pérez, P. How does the global electron density transfer diminish activation energies in polar cycloaddition reactions? A Molecular Electron Density Theory study. *Tetrahedron* **2017**, *73*, 1718–1724. [[CrossRef](#)]
28. Domingo, L.R.; Ríos-Gutiérrez, M.; Pérez, P. A Molecular Electron Density Theory Study of the Reactivity of Tetrazines in Aza-Diels–Alder Reactions. *RSC Adv.* **2020**, *10*, 15394–15405. [[CrossRef](#)]
29. Domingo, L.R.; Kula, K.; Ríos-Gutiérrez, M. Unveiling the Reactivity of Cyclic Azomethine Ylides in [3+2] Cycloaddition Reactions within the Molecular Electron Density Theory. *Eur. J. Org. Chem.* **2020**, 5938–5948. [[CrossRef](#)]
30. Houk, K.N.; González, J.; Li, Y. Pericyclic reaction transition states: Passions and punctilios, 1935–1995. *Acc. Chem. Res.* **1995**, *28*, 81–90. [[CrossRef](#)]
31. Sustmann, R.; Trill, H. Substituent Effects in 1,3-Dipolar Cycloadditions of Phenyl Azid. *Angew. Chem. Int. Ed. Engl.* **1972**, *11*, 838–840. [[CrossRef](#)]
32. Domingo, L.R.; Mar Ríos-Gutiérrez, M.; Silvi, B.; Pérez, P. The Mysticism of Pericyclic Reactions: A Contemporary Rationalisation of Organic Reactivity Based on Electron Density Analysis. *Eur. J. Org. Chem.* **2018**, 1107–1120. [[CrossRef](#)]
33. Domingo, L.R.; Ríos-Gutiérrez, M.; Pérez, P. A Molecular electron density theory study of the reactivity and selectivities in [3+2] cycloaddition reactions of C,N-dialkyl nitrones with ethylene derivatives. *J. Org. Chem.* **2018**, *83*, 2182–2197. [[CrossRef](#)]
34. El Ayouchia, H.B.; Lahoucine, B.; Anane, H.; Ríos-Gutiérrez, M.; Domingo, L.R.; Stiriba, S.-E. Experimental and Theoretical MEDT Study of the Thermal [3+2] Cycloaddition Reactions of Aryl Azides with Alkyne Derivatives. *ChemistrySelect* **2018**, *3*, 1215–1223. [[CrossRef](#)]
35. Becke, A.D. Density-functional thermochemistry. The role of exact Exchange. *J. Chem. Phys.* **1993**, *98*, 5648–5652. [[CrossRef](#)]
36. Lee, C.; Yang, W.; Parr, R.G. Development of the Colle-Salvetti correlation-energy formula into a functional of the electron density. *Phys. Rev. B* **1988**, *37*, 785–789. [[CrossRef](#)]
37. Hehre, M.J.; Radom, L.; Schleyer, P.v.R.; Pople, J. *Ab Initio Molecular Orbital Theory*; Wiley: New York, NY, USA, 1986.
38. Ess, H.; Houk, K.N. Theory of 1,3-Dipolar Cycloadditions: Distortion/Interaction and Frontier Molecular Orbital Models. *J. Am. Chem. Soc.* **2008**, *130*, 10187–10198. [[CrossRef](#)] [[PubMed](#)]

39. Schoenebeck, F.; Ess, D.H.; Jones, G.O.; Houk, K.N. Reactivity and Regioselectivity in 1,3-Dipolar Cycloadditions of Azides to Strained Alkynes and Alkenes: A Computational Study. *J. Am. Chem. Soc.* **2009**, *131*, 8121–8133. [[CrossRef](#)] [[PubMed](#)]
40. Barber, J.S.; Styduhar, E.D.; Pham, H.V.; McMahon, T.C.; Houk, K.N.; Garg, N.K. Nitron Cycloadditions of 1,2-Cyclohexadiene. *J. Am. Chem. Soc.* **2016**, *138*, 2512–2515. [[CrossRef](#)] [[PubMed](#)]
41. Domingo, L.R.; Ríos-Gutiérrez, M.; Emamian, S. Understanding the domino reaction between 1-diazopropan-2-one and 1,1-dinitroethylene. Amolecular electron density theory study of the [3+2] cycloaddition reactions of diazoalkanes with electron-deficient ethylenes. *RSC Adv.* **2017**, *7*, 15586–15595. [[CrossRef](#)]
42. Schlegel, H.B. Optimization of equilibrium geometries and transition structures. *J. Comput. Chem.* **1982**, *3*, 214–218. [[CrossRef](#)]
43. Schlegel, H.B. *Modern Electronic Structure Theory*; Yarkony, D.R., Ed.; World Scientific Publishing: Singapore, 1994.
44. Fukui, K. Formulation of the reaction coordinate. *J. Phys. Chem.* **1970**, *74*, 4161–4163. [[CrossRef](#)]
45. González, C.; Schlegel, H.B. Reaction path following in mass-weighted internal coordinates. *J. Phys. Chem.* **1990**, *94*, 5523–5527. [[CrossRef](#)]
46. González, C.; Schlegel, H.B. Improved algorithms for reaction path following: Higher-order implicit algorithms. *J. Chem. Phys.* **1991**, *95*, 5853–5860. [[CrossRef](#)]
47. Reed, A.E.; Weinstock, R.B.; Weinhold, F. Natural population analysis. *J. Chem. Phys.* **1985**, *83*, 735–746. [[CrossRef](#)]
48. Reed, A.E.; Curtiss, L.A.; Weinhold, F. Intermolecular interactions from a natural bond orbital, donor-acceptor viewpoint. *Chem. Rev.* **1988**, *88*, 899–926. [[CrossRef](#)]
49. Frisch, M.J.; Trucks, G.W.; Schlegel, H.B.; Scuseria, G.E.; Robb, M.A.; Cheeseman, J.R.; Scalmani, G.; Barone, V.; Petersson, G.A.; Nakatsuji, H.; et al. *Gaussian 16, Revision A.03*; Gaussian, Inc.: Wallingford, CT, USA, 2016.
50. Noury, S.; Krokidis, X.; Fuster, F.; Silvi, B. Computational tools for the electron localization function topological analysis. *Comput. Chem.* **1999**, *23*, 597–604. [[CrossRef](#)]
51. Dennington, R.; Keith, T.A.; Millam, J.M. *GaussView, Version 6.0*; Semichem Inc.: Shawnee Mission, KS, USA, 2016.
52. Ahrens, J.; Geveci, B.; Law, C. *ParaView: An End-User Tool for Large Data Visualization, Visualization Handbook*; Elsevier: Amsterdam, The Netherlands, 2005; ISBN 13: 978-0123875822.
53. Ayachit, U. *The ParaView Guide: A Parallel Visualization Application*; Kitware: New York, NY, USA, 2015; ISBN 978-1930934306.
54. Silvi, B.; Savin, A. Classification of chemical bonds based on topological analysis of electron localization functions. *Nature* **1994**, *371*, 683–686. [[CrossRef](#)]
55. Domingo, L.R.; Sáez, J.A. Understanding the Electronic Reorganization along the Nonpolar [3+2] Cycloaddition Reactions of Carbonyl Ylides. *J. Org. Chem.* **2011**, *76*, 373–379. [[CrossRef](#)] [[PubMed](#)]
56. Huisgen, R. 1,3-Dipolar cycloadditions. 76. Concerted nature of 1,3-dipolar cycloadditions and the question of diradical intermediates. *J. Org. Chem.* **1976**, *41*, 403–419. [[CrossRef](#)]
57. Firestone, R.A. Mechanism of 1,3-dipolar cycloadditions. *J. Org. Chem.* **1968**, *33*, 2285–2290. [[CrossRef](#)]
58. Parr, R.G.; Pearson, R.G. Absolute hardness: Companion parameter to absolute electronegativity. *J. Am. Chem. Soc.* **1983**, *105*, 7512–7516. [[CrossRef](#)]
59. Chamorro, E.; Duque-Noreña, M.; Gutiérrez-Sánchez, N.; Rincón, E.; Domingo, L.R. A close look to the oxaphosphetane formation along the Wittig reaction: A [2+2] cycloaddition? *J. Org. Chem.* **2020**, *85*, 6675–6686. [[CrossRef](#)]

Publisher's Note: MDPI stays neutral with regard to jurisdictional claims in published maps and institutional affiliations.



© 2020 by the authors. Licensee MDPI, Basel, Switzerland. This article is an open access article distributed under the terms and conditions of the Creative Commons Attribution (CC BY) license (<http://creativecommons.org/licenses/by/4.0/>).